Journal of Nuclear Materials 390–391 (2009) 119–122

Contents lists available at ScienceDirect

Journal of Nuclear Materials

journal homepage: www.elsevier.com/locate/jnucmat

Simulation of redeposition of carbon/hydrocarbon on a material surface with castellated structures

K. Inai [a,*], K. Ohya [b], Y. Tomita [c], A. Kirschner [d], A. Litnovsky [d], T. Tanabe [e]

[a] Graduate School of Advanced Technology and Science, The University of Tokushima, Minamijosanjima 2-1, Tokushima 770-8506, Japan
[b] Institute of Technology and Science, The University of Tokushima, Tokushima 770-8506, Japan
[c] Department of Simulation Science, National Institute for Fusion Science, Toki 509-5292, Japan
[d] Institut für Energieforschung-Plasmaphysik, Forschungszentrum Jülich, 52425 Jülich, Germany
[e] Interdisciplinary Graduate School of Engineering Science, Kyushu University, Fukuoka 812-8581, Japan

ARTICLE INFO

PACS:
52.40.Hf
52.55.Rk
52.65.Pp

ABSTRACT

Castellated armor tiles are anticipated to withstand intense heat fluxes on the plasma-facing divertors and limiters. We performed a simulation of the transport and the redeposition of carbon and hydrocarbons on the castellated structure in order to study the mechanisms of redeposition in the gaps using realistic plasma penetration in the gap and their energy- and species-dependent reflection on the surface. The calculated profile for the chemical sputtering, but not the physical sputtering, reproduces the experimental deposition profile within an ITER-like castellation geometry in TEXTOR. From the simulation, we proposed a new castellation geometry. The optimization of the shape of the castellated unit cell is very likely to work to minimize the redeposition rate in the gaps.

1. Introduction

Castellated armor tiles on the first wall and the divertor are anticipated to ensure thermo-mechanical durability. Experiments with an ITER-like castellation geometry in TEXTOR [1], are studying the fuel retention and impurity transport in gaps. To investigate the mechanisms of redeposition in the gaps and discuss the effectiveness of deposition mitigation techniques, we performed a simulation study of transport and redeposition of carbon and hydrocarbons where realistic plasma penetration in the gap and their energy- and species-dependent reflection on the surface are taken into account.

2. Simulation of carbon/hydrocarbon redeposition in the gaps

Schematic views of the tile and gap configuration used for our calculation are presented in the insets of Fig. 1. The gaps orient toward the toroidal and poloidal directions, which are named as toroidal and poloidal gaps, respectively. A homogeneous plasma with constant electron and ion temperature ($T_e = T_i$) and the electron density, which is assumed to fulfill the Boltzmann relation, contacts the top surface of the tile. The thickness of the plasma is 10 cm. The sides of the simulation cell have a periodic boundary. CH_4 molecules with a Maxwellian velocity distribution corresponding to a temperature of 0.1 eV (1160 K) are generated randomly from whole area of the top surface. The released molecules experience complex collision reactions in the plasma. The rate coefficients for electron-impact ionization, dissociation, dissociative recombination, proton-impact ionization and charge exchange processes of CH_4 and fragments are calculated using fitting formulae taken from Janev and Reiter [2]. The elastic scattering of the resultant atoms or ions by ambient hydrogen atoms is considered via the hard sphere collision model. Details of our simulation model are provided in [3].

Reflection/sticking coefficients at the tile surface are considered by using classical molecular dynamics (MD) simulation [4]. We used the interaction potential based on analytic bond-order scheme, which was developed by Juslin et al. [5] for the ternary system W–C–H. In our MD simulation the hydrogenated and amorphized graphite was prepared as a starting surface by bombardment with carbon ($E = 0.025$ eV) and hydrogen ($E = 1$ eV). Since the direct coupling of the transport/redeposition code with the MD is very time-consuming, the database of the energy- and species-dependent reflection coefficients which are prepared using the MD are employed in the transport/redeposition code. The hydrocarbons are incident on the surface at the angle of 45° against the surface normal.

If a particle produced by a reaction is charged in the plasma, it gyrates receiving various forces, such as friction and thermal gradient forces [6], cross-field diffusion [7], and sheath acceleration. However, there is no thermal gradient force due to the constant plasma. To simplify complex sheath structure in the gap, we use the Brooks model [8] with following modification:

* Corresponding author.
E-mail address: ken-171@ee.tokushima-u.ac.jp (K. Inai).

0022-3115/$ - see front matter © 2009 Elsevier B.V. All rights reserved.
doi:10.1016/j.jnucmat.2009.01.136

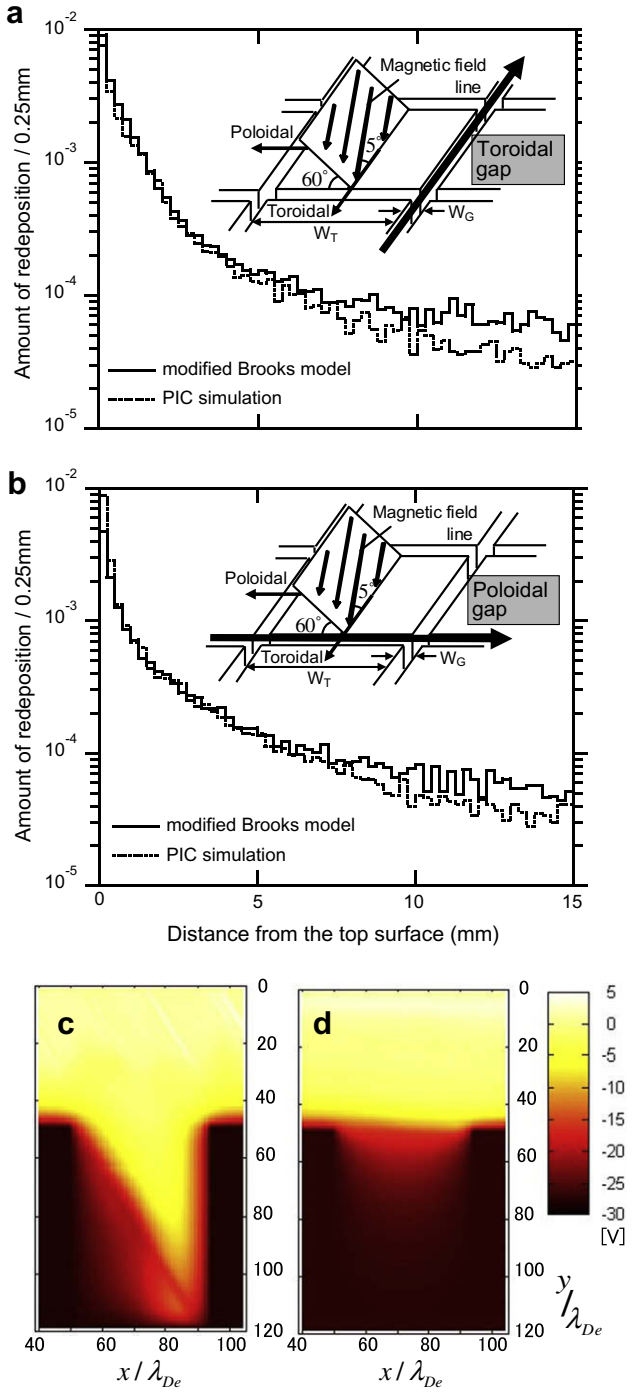

Fig. 1. The amount of redeposition on the side surface of (a) toroidal and (b) poloidal gaps as a function of the distance from the top surface. Two side deposition profiles are summed. Schematic view of the tile and gap configuration for toroidal and poloidal gaps between the tiles (W_T = 20 mm, W_G = 1 mm, D = 15 mm) and the electric potential distribution calculated by using PIC simulation for (c) toroidal and (d) poloidal gaps ($n_e = 10^{18}$ m^{-3}, T_e = 10 eV, B = 5 T, $\lambda_{De} = 23.5$ μm) are shown.

$$\phi(\vec{r}) = \phi_0 \exp[-l(\vec{r})/\lambda],$$
$$\lambda = \delta_1 \sin\beta\lambda_{Li} + \delta_2(1 - \sin\beta)\lambda_{De},$$

where $\phi_0 \approx -3kT_e$, β is the angle of the magnetic field line from the surface normal, λ_{Li} is gyro-radius of the plasma ion, λ_{De} is the Debye length and δ_1, δ_2 are the arbitrary constants ($\delta_1, \delta_2 = 1$). The distance from a point in the sheath to the surface, l, is taken to be the distance along the curved electric field lines toward the sides and bottom of the gap. The decay of the plasma density in the gap is assumed to be dependent on the sheath potential according to the Boltzmann relation.

For benchmarking, we also developed a particle-in-cell (PIC) simulation code, which is 3-dimensional in velocity space and 2-dimensional in real space. The velocity distribution of plasma ions is a shifted Maxwellian with velocity cut-off that satisfies the generalized Bohm criterion at the electrostatic sheath entrance, whereas the injected plasma electrons are assumed to be Maxwellian. The electric potential distribution in the vicinity of the gaps is shown in Fig. 1.

3. Result and discussion

3.1. General study for the redeposition in the toroidal and poloidal gaps

Fig. 1 shows the amount of redeposition on the side surface of (a) toroidal and (b) poloidal gaps as a function of the distance from the top surface. The plasma density and the sheath potential profiles are calculated by the PIC simulation and using the modified Brooks model. Since carbon and hydrocarbon ions are drawn into the gap along the electric field lines they are mostly redeposited in the vicinity of the gap entrance. According to the modified Brooks model, the differences of the inclination angles of the magnetic field between the poloidal and the toroidal gaps cause strong asymmetry of the sheath potentials between them. Since the reflection coefficients for ions and neutrals are different [9], the redeposition profile in the gap sides is influenced by the plasma penetration due to the sheath acceleration of ion species. In the toroidal gap, there is a deep penetration of the plasma into the gap, which causes the local increase in the amount of redeposition in the vicinity of the top surface (<2 mm). On the other hand, there is the shallow penetration in the poloidal gap. Since the plasma cannot decay enough for our modified Brooks model, the Boltzmann relation also should be modified in the gap.

3.2. Modeling for castellated test limiter in TEXTOR

For a castellated test limiter experiment in TEXTOR [1] we performed the simulation of transport and redeposition of hydrocarbons and carbons sputtered physically. Plasma deuterium ions with Maxwellian velocity distribution are generated at the top area of simulation volume, move along the magnetic field lines with gyration and bombard the castellated limiter. From the bombarded point of the limiter surface, a Carbon atom with a Thompson distribution or a CH_4 molecule with Maxellian distribution is released. Carbon atoms and ions, which return to the surface after the migration in the background plasma, are deposited or reflected with an emission angle according to the EDDY code calculation [10], whereas the hydrocarbon reflection is calculated using the database prepared by the MD calculation. From PIC simulation, there is the shallow penetration in the poloidal gap. Therefore, we assumed the CH_4 and fragments do not collide with plasma electrons and ions at the plasma-shadowed area. Furthermore, sheath acceleration occurs toward the gap entrance and tile surface; however, it does not occur in the gap.

Fig. 2 shows the observed C redeposition profiles [1] and the calculated profile in the poloidal gaps. Due to clear comparison between the calculated and the observed profiles, the observed density of redeposited carbon atoms is reduced by a constant density around the bottom of the gap. The calculated amount of redeposition is quantitatively compared with the observed areal density of redeposited carbon atoms. The calculated redeposition profile in the rectangular cell (the inset in Fig. 2(a)) reproduces the high peak

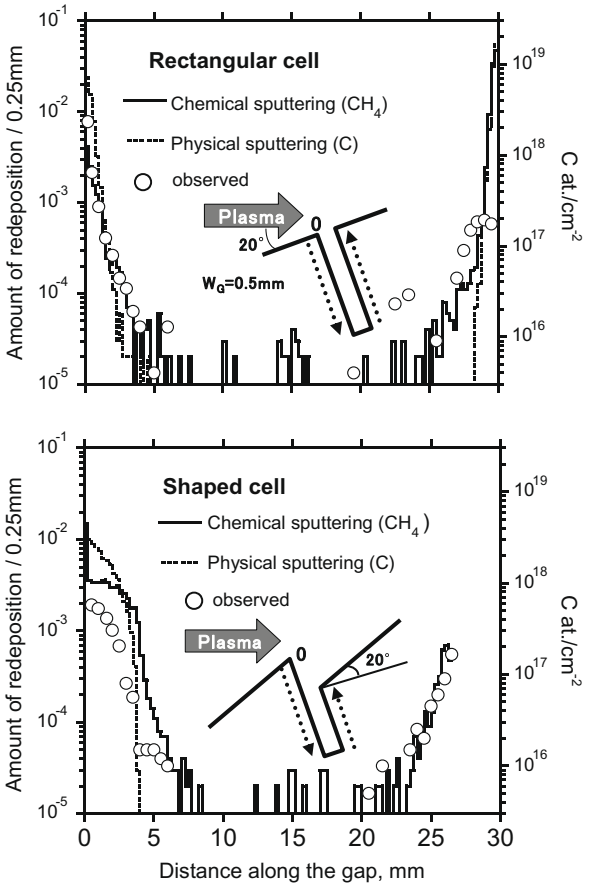

Fig. 2. The observed C redeposition profiles [1] and the calculated profiles in the poloidal gaps of (a) the rectangular cell and (b) shaped cell ($W_T = 10$ mm, $n_e = 6 \times 10^{18}$ m^{-3}, $T_e = 20$ eV, $B = 5$ T). The beginning of abscissa axis corresponds to the top surface of the plasma-shadowed side. The observed density of redeposited carbon atoms is reduced by a constant density around the bottom of the gap.

values near the plasma-shadowed edge. The reflected particle and emitted one from the rim are redeposited there. The particles transported from top surfaces are redeposited on the plasma-open side. However, the redeposition layer is bombarded with the background plasma, so that C amount is reduced there. Furthermore the

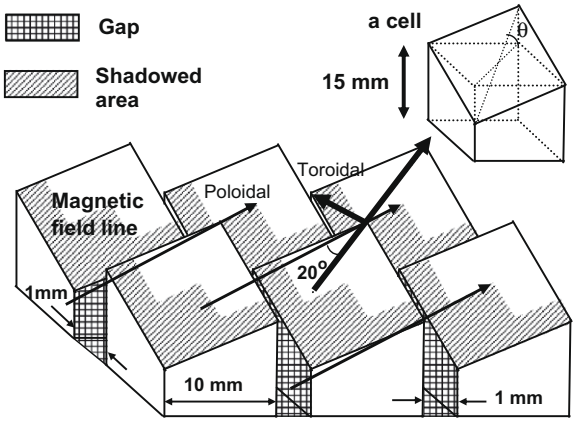

Fig. 3. Schematic views of the unit cell and the gap configuration for new castellation geometry. In order to hide both poloidal and toroidal gaps from direct access, the gaps are oblique to both the toroidal and the poloidal directions, whereas the tile surface is tilted with respect to the toroidal direction by angle, θ.

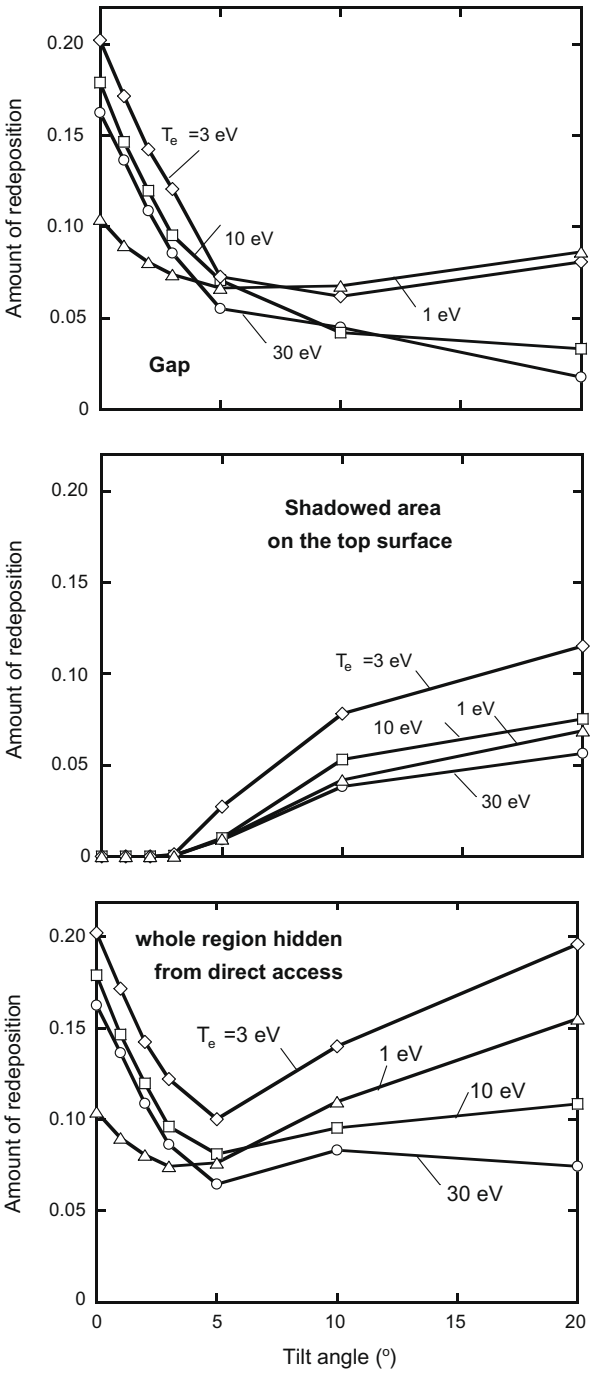

Fig. 4. The amount of redeposition of hydrocarbons/carbon on (a) only the gap sides, (b) the shadowed area on the top surface and (c) the whole region depending on the tilt angle of the tile surface and the plasma temperature ($n_e = 10^{20}$ m^{-3}).

profiles for the chemical sputtering decay on a longer range than them for the physical sputtering. Because carbon ions transported from top surfaces are easy to redeposit at the plasma-open side due to their high energy, whereas most of hydrocarbon reflects at the side surface. The calculated profile for the hydrocarbons reproduces the experimental profile in TEXTOR [1]. In the shaped cell, unless the particles are repeatedly reflected from the top surfaces of the cell, it cannot redeposit directly in the gaps. Therefore the redeposition profiles are broader. The shaped cell used for our simulation has a sharp edge at the plasma-shadowed side, but the cell edge used in the experiment is cut. Although it is difficult to

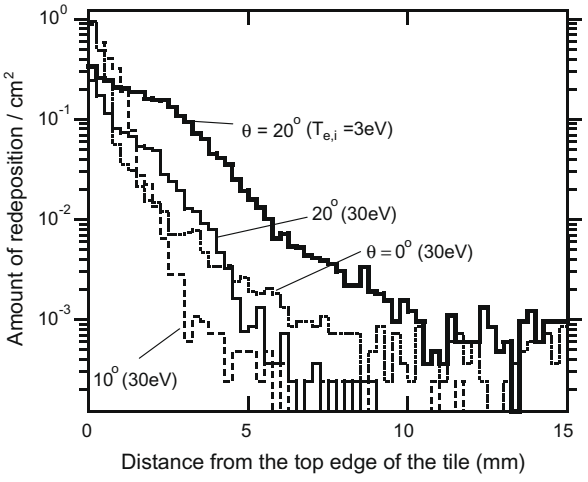

Fig. 5. The amount of redeposition of carbon/hydrocarbon as a function of the distance from the top edge of the tile, depending on the tilt angle of the tile surface and the plasma temperature.

compare between the calculation and the experiment, the particles emitted from the top surface are locally redeposited at the upper part of the gap side (<4 mm) for both. Anyway, the gaps between the shaped cells are not directly bombarded so that the redeposition in the gap is suppressed.

3.3. Analysis of influence of gap geometry

In a previous paper [3], the castellated structure with the cells tilted against the toroidal direction was studied in order to minimize the redeposition in poloidal gaps. In this study, in order to hide both of the poloidal and the toroidal gaps from direct access, the gaps are oblique to both the toroidal and the poloidal directions, whereas the tile surface is tilted with respect to the toroidal direction by angle, θ (Fig. 3). As shown in Fig. 4 because of tilt of the unit cell, the redeposition in the gap is strongly suppressed. With further increasing the tilt angle θ, the tile regions (the shadowed areas of the top surface) hidden from direct access have a larger surface area so that the amount of redepostion increases. Furthermore, with decreasing plasma temperatures the amount of redeposition increases due to dominant redeposition of neutral species. However, at the lowest plasma temperatures ($\sim$1 eV), many hydrocarbons are transported over the simulation volume and the amount of redeposition decreases. Fig. 5 shows the amount of redeposition relative to the area as a function of the distance from the top edge. With increasing tilt angle θ, the redeposition of carbon/hydrocarbon is enhanced at the upper part of the plasma-shadowed gap, whereas due to the hidden gaps from direct access it is suppressed in the deep regions of the gap. At a low plasma temperature (3 eV) the redeposition of the neutral species with the high reflection coefficient are dominant, so that the redeposition profile is broader. The reduction of the areas directly exposed to plasmas with the optimization of the shape of the castellated unit cell is very likely to work to minimize the redeposition rate in the gaps of the castellated structure, ex., at the angle of $\theta = 5°$. The optimized angle is related to the geometry of the tiles.

4. Conclusion

In order to investigate the mechanisms of redeposition and study the effectiveness of deposition mitigation techniques we performed a simulation study of transport and redeposition of carbon and hydrocarbons on the castellated structure. We applied a model with a modification to simplify complex sheath and plasma profiles around the gap and such calculation was compared to a PIC calculation. The calculated profile for the chemical sputtering, but not the physical sputtering, reproduces the redeposition profile observed with an ITER-like castellation geometry in TEXTOR. Since the gaps between the shaped cells with tilted surface are not directly bombarded with the plasma, the redeposition in the gap is strongly suppressed. From the simulation, we proposed a new castellation geometry. The optimization of the shape of the castellated unit cell is very likely to work to minimize the redeposition rate in the gaps of the castellated structure due to the reduction of the areas directly exposed to plasmas.

Acknowledgement

This work was supported by KAKENHI (19055005).

References

[1] A. Litnovsky et al., J. Nucl. Mater. 390–391 (2009) 900.
[2] R.K. Janev, D. Reiter, Rep. Forschungszentrum Jülich, Jül-3966, 2002.
[3] K. Inai, K. Ohya, Contrib. Plasma Phys. 48 (1–3) (2008) 275.
[4] K. Ohya, Y. Kikuhara, K. Inai, A. Kirschner, D. Borodin, A. Ito, H. Nakamura, T. Tanabe, J. Nucl. Mater. 390–391 (2009) 72.
[5] N. Juslin, P. Erhart, P. Träskelin, J. Nord, K. Henriksson, E. Salonen, K. Nordlund, K. Albe, J. Appl. Phys. 98 (2005) 123520.
[6] P.C. Stangeby, The Plasma Boundary of Magnetic Fusion Devices, IOP, Bristol, 2000. p. 296.
[7] K. Shimizu, H. Kubo, T. Takizuka, et al., J. Nucl. Mater. 220–222 (1995) 410.
[8] J.N. Brooks, Phys. Fluid B 2 (1990) 1858.
[9] K. Inai, K. Ohya, J. Nucl. Mater 363–365 (2007) 915.
[10] Y. Hamada, S. Ebisu, K. Ohya, Jpn. J. Appl. Phys. 43 (2007) 6385.